Historical Land-Cover Change Impacts on Climate: Comparative Assessment of LUCID and CMIP5 Multimodel Experiments

QUENTIN LEJEUNE, SONIA I. SENEVIRATNE, AND EDOUARD L. DAVIN

Institute for Atmospheric and Climate Science, ETH Zürich, Zürich, Switzerland

(Manuscript received 11 March 2016, in final form 7 September 2016)

ABSTRACT

During the industrial period, many regions experienced a reduction in forest cover and an expansion of agricultural areas, in particular North America, northern Eurasia, and South Asia. Here, results from the Land-Use and Climate, Identification of Robust Impacts (LUCID) and CMIP5 model intercomparison projects are compared in order to investigate how land-cover changes (LCC) in these regions have locally impacted the biophysical land surface properties, like albedo and evapotranspiration, and how this has affected seasonal mean temperature as well as its diurnal cycle. The impact of LCC is extracted from climate simulations, including all historical forcings, using a method that is shown to capture well the sign and the seasonal cycle of the impacts diagnosed from single-forcing experiments in most cases.

The model comparison reveals that both the LUCID and CMIP5 models agree on the albedo-induced reduction of mean winter temperatures over midlatitudes. In contrast, there is less agreement concerning the response of the latent heat flux and, subsequently, mean temperature during summer, when evaporative cooling plays a more important role. Overall, a majority of models exhibit a local warming effect of LCC during this season, contrasting with results from the LUCID studies. A striking result is that none of the analyzed models reproduce well the changes in the diurnal cycle identified in present-day observations of the effect of deforestation. However, overall the CMIP5 models better simulate the observed summer daytime warming effect compared to the LUCID models, as well as the winter nighttime cooling effect.

1. Introduction

Since the beginning of the Industrial Revolution, the world's population has tremendously increased, thereby strengthening the demand for more agricultural land. Consequently, forests and natural grasslands have been replaced by crops and pastures over large parts of the world (Ramankutty and Foley 1999; Foley et al. 2005; Pongratz et al. 2008; Klein Goldewijk et al. 2011; Hurtt et al. 2011). This mostly occurred over the eastern part of North America and the Great Plains, Northern Eurasia, and less extensively over India, eastern Asia, and South America, as well as more recently in tropical areas. These historical land-cover changes (LCC) have impacted climate through both biogeochemical effects (i.e., through an increase in atmospheric carbon dioxide concentration) and biogeophysical effects (i.e., modifications of the biophysical properties of the land surface) (Brovkin et al. 2004; Findell et al. 2007; Pongratz et al. 2010; de Noblet-Ducoudré et al. 2012; Kumar et al. 2013).

The Land-Use and Climate, Identification of Robust Impacts (LUCID) model intercomparison project specifically aims to quantify these biogeophysical effects on climate. De Noblet-Ducoudré et al. (2012) found that six of the seven general circulation models (GCMs) taking part in LUCID indicate an all-year cooling through biogeophysical mechanisms over the affected midlatitudinal regions (North America and Eurasia) during the industrial era, which almost canceled out locally the warming driven by the concomitant increase in atmospheric CO_2 concentration. They identified the higher albedo of the anthropogenic croplands and pastures compared to

Denotes content that is immediately available upon publication as open access.

Supplemental information related to this paper is available at the Journals Online website: http://dx.doi.org/10.1175/JCLI-D-16-0213.s1.

Corresponding author e-mail: Quentin Lejeune, quentin.lejeune@env.ethz.ch; Edouard L. Davin, edouard.davin@env.ethz.ch

Publisher's Note: This article was revised on 27 April 2017 to correct an editing error in the second paragraph of the Introduction.

DOI: 10.1175/JCLI-D-16-0213.1

primary forests as an important cooling mechanism in each model, particularly in winter over snow-covered areas. However, de Noblet-Ducoudré et al. (2012) underlined the low intermodel consistency on the responses of the latent and sensible heat fluxes to historical modifications of the albedo, roughness length, leaf area index, root depth, and stomatal resistance of the vegetation.

Phase 5 of the Coupled Model Intercomparison Project (CMIP5) offers an opportunity to reassess the climatic impacts of LCC in the context of more recent, fully coupled GCMs. Indeed, a transient LCC forcing based on the reconstruction of Hurtt et al. (2011) was included in more than 15 of the CMIP5 models. However, the classical approach to extract LCC effects based on factorial experiments (e.g., by comparing experiments with and without the LCC forcing) is not applicable to CMIP5 since most models only provide so-called all-forcings experiments. To overcome this challenge, Kumar et al. (2013) developed a methodology to extract the LCC forcing from such experiments. It consists in comparing the evolution of climatic variables over neighboring grid cells, which experienced different rates of LCC but were similarly affected by other forcings. Similar approaches had beforehand already been applied to observations (e.g., McPherson et al. 2004; Ge 2010; Loarie et al. 2011; Wickham et al. 2012). Interestingly, Kumar et al. (2013) found a much lower model agreement about the impact of historical LCC on summer temperature than in LUCID studies. Only about half of the models they considered indeed showed a mean cooling effect over North America, while the other half showed a mean warming effect. They evaluated the reconstruction method that they developed by comparing its results to those of the factorial experiment approach, but this comparison remained limited to one single model and only two ensemble simulations. Even if they found a good similarity between both methodologies, it does not ensure that this result can be generalized to all models. Moreover, Kumar et al. (2013) chose to focus on the consequences of LCC for summer temperature, even if the LUCID studies revealed effects of at least similar magnitude in other seasons (Boisier et al. 2012; de Noblet-Ducoudré et al. 2012). Besides, some recent observational studies demonstrated that the impact of deforestation on air and surface temperatures over midlatitudes has an opposite sign during daytime and nighttime (e.g., Lee et al. 2011; Vanden Broucke et al. 2015; Li et al. 2015), a feature which was mostly overlooked in previous modeling studies.

Consequently, in this study we intend to answer three research questions:

- Is the reconstruction method based on Kumar et al. (2013) able to assess the historical LCC impacts on albedo, latent heat flux and surface air temperature, and are its estimates comparable to those of the method using factorial experiments? (section 3a)
- Do the CMIP5 models confirm the results from the LUCID project regarding the impact of LCC on surface air temperature during the industrial period? (section 3b)
- Are model results consistent with present-day observations of the impact of deforestation on temperature, and especially its diurnal cycle? (section 3c)

2. Data and methods

a. Description of the reconstruction method

To extract the LCC signal from single transient simulations, we employ a method based on Kumar et al. (2013) with some modifications. This method, illustrated in Fig. 1, assumes that LCC constitute a spatially heterogeneous forcing with essentially local climate impacts (i.e., this method cannot be applied to simulations with large-scale homogeneous forcings and will work only to the extent that local effects outweigh possible remote effects). In contrast, other forcings like greenhouse gases (GHG) are assumed to have a more homogeneous and larger-scale impact on climate.

For a given model, we therefore separate between grid cells for which the mean tree fraction between a preindustrial and a present-day period has decreased by at least 15% (the high-LCC grid cells) and the others (the low-LCC grid cells). In a next step, for each high-LCC grid cell we look at a bigger box of 5×5 grid cells centered over it. Then, to disentangle the impact of LCC from that of other forcings between the preindustrial and present-day periods in this high-LCC grid cell, we compute the difference in the mean temporal changes in climatic conditions over the high-LCC grid cells and those over the low-LCC grid cells contained within the corresponding bigger box. Looking at temporal changes also allows us to cancel out at least partly possible spurious effects due to climatic gradients unrelated to LCC within a bigger box (e.g., due to topography). We require each bigger box to contain at least three high-LCC and three low-LCC grid cells (and at least eight in total) and also the ratio of the number of its high-LCC grid cells over the total number of its land grid cells to be as close as possible to 0.5. If these criteria are not fulfilled, the size of the bigger boxes is increased to 7×7 or even 7×9 grid cells. We found that using this protocol compared to a fixed bigger box increases the ability of the reconstruction method to disentangle the impact of LCC from climate changes due to other forcings and internal variability (see the next section). The choice of a threshold of 15% to

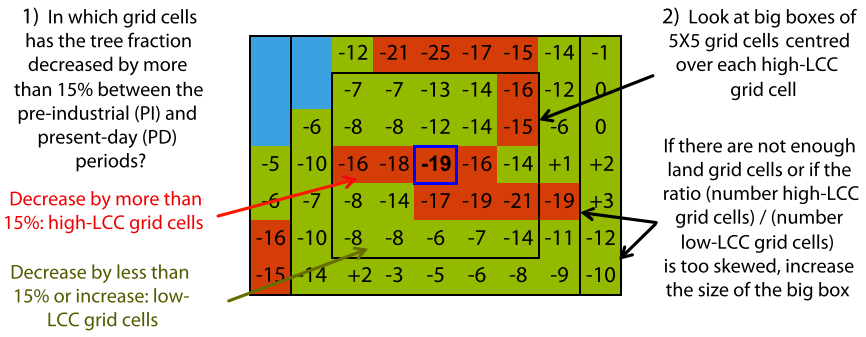

3) To extract the LCC impact on a climate variable X over a given LCC grid cell: within the corresponding big box, compute the average changes in this variable between PD and PI over high-LCC grid cells minus those over low-LCC grid cells

$$\text{LCC impact} = \overline{\Delta X}^{\text{high-LCC}}_{\text{PI}\to\text{PD}} - \overline{\Delta X}^{\text{low-LCC}}_{\text{PI}\to\text{PD}}$$

FIG. 1. Illustration of the methodology employed to reconstruct the impact of land-cover changes in the model grid cell highlighted in blue, using all-forcings simulations. The numbers indicate the change in tree fraction between the preindustrial and present-day periods in each grid cell. Red grid cells are high-LCC grid cells in which the tree fraction has decreased by more than 15%, while green grid cells are low-LCC grid cells in which the tree fraction has decreased by less than 15% or increased. Light blue grid cells are ocean or lake grid cells.

separate between high- and low-LCC grid cells was also made in order to optimize the method (more details are also given in the next section).

Contrary to Kumar et al. (2013), we did not conduct our analysis on model data regridded to a common 2.5° × 2.5° resolution but kept them in their native grid, nor did we separate high- from low-LCC grid cells in CMIP5 simulations based on the increase in crop cover according to the dataset from Hurtt et al. (2011). We have made these decisions because 1) deforestation leads to a clearer climatic signal than the expansion of croplands, since forests exhibit a distinct influence on the surface climatic variables compared to short vegetation types that are typical of agricultural areas, whereas crops overall behave more similarly to natural grasslands (Ambrose and Sterling 2014; Zhao and Jackson 2014); 2) we found that the LCC impacts could be better disentangled from those of other forcings and internal variability if the method is based on the decrease in tree fraction rather than on the increase in crop fraction; 3) even if they were based on vegetation datasets that are the same for each intercomparison project, the analyzed models interpret those differently and thus did not uniformly prescribe the LCC forcing; and 4) we observed that after regridding the reconstruction method would extract LCC impacts that were somewhat attenuated. More developed justifications for these methodological choices are provided in the next section (section 3a), following a comparison of the reconstruction method with that using factorial experiments.

b. LUCID simulations

The LUCID project aimed to identify the robust biogeophysical impacts of LCC that have occurred since the mid-nineteenth century. We have analyzed six models from this project, listed in Table 1. They all ran four experiments with five 30-yr ensemble simulations each and

TABLE 1. List of the LUCID models analyzed in this study.

Model name	Institution	Reference	Resolution (lat × lon)	Ensemble size
ARPEGE	Centre National de la Recherche Météorologique	Salas-Mélia et al. (2005)	64 × 128	5
CCAM	Commonwealth Scientific and Industrial Research Organization	McGregor and Dix (2008)	91 × 180[a]	5
CCSM	National Center for Atmospheric Research	Collins et al. (2006)	96 × 144	5
ECHAM5	Max-Planck-Institut für Meteorologie	Roeckner et al. (2006)	91 × 180[a]	5
IPSL	L'Institut Pierre-Simon Laplace	Marti et al. (2010)	72 × 96	5
SPEEDY	International Centre for Theoretical Physics	Strengers et al. (2010)	91 × 180[a]	5

[a] Interpolated data were analyzed since original data stored in the native grid were partly missing.

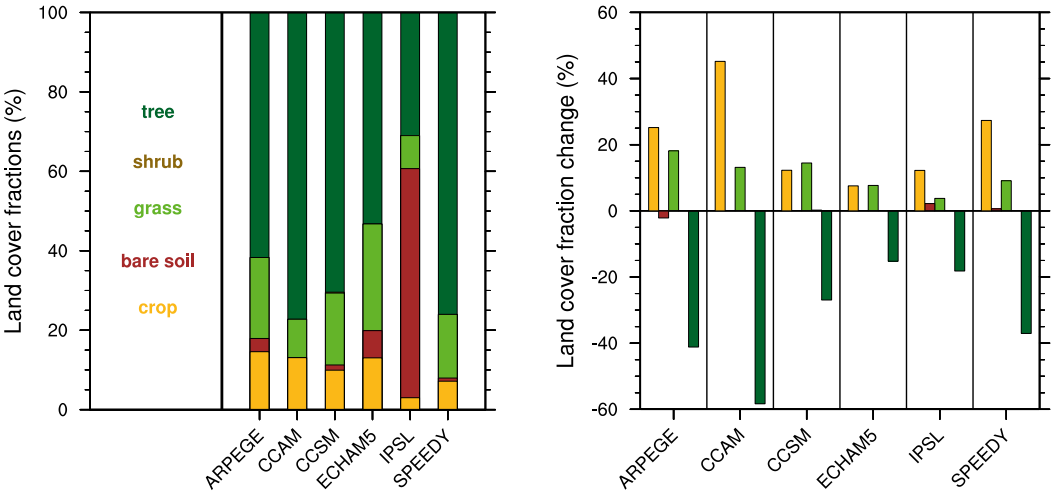

FIG. 2. Land-cover changes in the LUCID models in North America (30°–60°N, 230°–310°E). (left) Mean fraction of each land-cover type over high-LCC grid cells in the 1870 vegetation maps (corresponding to preindustrial conditions). (right) Changes in land-cover fractions between the vegetation maps of 1870 and those of 1992 (representative of present-day conditions) over high-LCC grid cells, minus those same changes over low-LCC grid cells. A negative value for the tree bar means, for example, that the tree fraction has decreased more over high- than over low-LCC grid cells between the preindustrial and present-day periods.

used prescribed interannually and seasonally varying sea surface temperatures (SSTs) and sea ice extent. Each model was provided with a map showing the change in the extent of both crops and pastures between 1870 (preindustrial conditions) and 1992 (present-day conditions). This map was obtained by combination of the crop area reconstructed by Ramankutty and Foley (1999) and the pasture area from Klein Goldewijk (2001). It was then adapted by each model center depending on their "natural" vegetation distribution as well as their own interpretation of these prescribed land-use transitions. For each model, the mean gridcell fraction covered by each land-cover type over the high-LCC grid cells during the preindustrial period is shown in Fig. 2a for North America (30°–60°N, 230°–310°E), while the differences in the change in these fractions from the preindustrial to the present-day periods between the high- and low-LCC grid cells are shown in Fig. 2b. In the body of this article we show only results for North America, but respective analyses for Eurasia (40°–60°N, 20°–100°E) and South Asia (5°–35°N, 65°–115°E) are systematically provided in the supplemental material (SM; see its Figs. S2–S5 in this case).

The first (second) experiment was called PD (PI) and used land cover, GHG concentrations, SSTs, and sea ice extent reflecting present-day (preindustrial) conditions. A third experiment (PDv) used the same forcings as PD, apart from land cover, which was set to preindustrial conditions. Similarly, the fourth experiment (PIv) was conducted by prescribing the same forcings as in PI, except for land cover, which was set to present-day conditions. To isolate the climate impacts of historical LCC from those of other forcings that evolved concomitantly, the LUCID studies looked at the difference between two experiments differing only in terms of land-cover map under both preindustrial and present-day GHG concentrations and SSTs [i.e., PIv − PI and PD − PDv; see, e.g., Pitman et al. (2009); de Noblet-Ducoudré et al. (2012); Boisier et al. (2012)]. However in this study, we use a reconstruction algorithm that aims to isolate the climate impacts of LCC in simulations where both land cover and other forcings are varying. In the case of LUCID simulations, we hence apply it to the difference between the PD and PI experiments. In order to quantify to which extent this reconstruction method may also capture climate variations not due to LCC, we also apply this algorithm to the differences between simulations sharing the same land-cover map but differing in terms of GHG concentrations, SSTs, and sea ice extent (PD − PIv and PDv − PI).

c. *CMIP5 simulations*

Many models involved in CMIP5 included LCC as a forcing in their historical all-forcings simulations, which covered the 1860–2005 period (Taylor et al. 2012). We have analyzed 11 of these models (listed in Table 2), selecting only those that provided land-cover information, as well as surface air temperature, albedo, and latent heat flux outputs at monthly resolution. They are all coupled models that compute SSTs interactively and simulate land surface processes explicitly. To represent historical LCC, they adapted the dataset developed by Hurtt et al.

TABLE 2. List of the CMIP5 models analyzed in this study.

Model name	Institution	Reference	Resolution on land (lat × lon)	Ensemble size
CanESM2	Canadian Centre for Climate Modeling and Analysis	Arora et al. (2011)	64 × 128	5
CCSM4	National Center for Atmospheric Research	Gent et al. (2011)	192 × 288	6
CESM1(CAM5)	National Center for Atmospheric Research	http://www2.cesm.ucar.edu/models	192 × 288	3
CESM1 (FASTCHEM)	National Center for Atmospheric Research	http://www2.cesm.ucar.edu/models	192 × 288	3
GFDL CM3	NOAA Geophysical Fluid Dynamics Laboratory	http://www.gfdl.noaa.gov	90 × 144	5
HadGEM2-ES	Met Office Hadley Centre	Collins et al. (2008)	145 × 192	4
IPSL-CM5A-LR	L'Institut Pierre-Simon Laplace	http://icmc.ipsl.fr; Dufresne et al. (2013)	96 × 96	6
IPSL-CM5A-MR	L'Institut Pierre-Simon Laplace	http://icmc.ipsl.fr; Dufresne et al. (2013)	143 × 144	3
MPI-ESM-LR	Max-Planck-Institut für Meteorologie	Raddatz et al. (2007); Marsland et al. (2003)	96 × 192	3
MPI-ESM-MR	Max-Planck-Institut für Meteorologie	Raddatz et al. (2007); Marsland et al. (2003)	96 × 192	3
NorESM1-M	Norwegian Climate Centre	Bentsen et al. (2013)	96 × 144	3

(2011) based on Klein Goldewijk et al. (2011), which provides maps of the land-use states and transitions between cropland, pasture, primary land, and secondary (recovering) land between 1500 and 2005 at 0.5° resolution. We have used the reconstruction method to extract the climate impacts of historical LCC between two 30-yr time slices of each all-forcings simulation: 1862–1891 (preindustrial period) and 1975–2004 (present-day period). The mean gridcell fraction covered by each land-cover type over the high-LCC grid cells in North America during the preindustrial period is shown in Fig. 3a, while Fig. 3b shows how it evolved over the high-LCC grid cells compared to the low-LCC ones by the present-day period.

3. Results and discussion

a. Part 1: Evaluation of the reconstruction method

1) Comparison with the factorial experiment approach

Because of their specific experimental design, the LUCID simulations are appropriate to compare the reconstruction method and the factorial experiment approach. The former can indeed be applied to the difference between LUCID simulations where both the land cover and the CO_2/SST/sea ice forcings differ (PD − PI). As for the latter, which consists of comparing a simulation forced by LCC only with a control (or an all-forcings simulation with another one forced by all forcings except LCC), one can apply it to the difference between two simulations differing only in terms of vegetation map (PD − PDv or PIv − PI). Therefore, in this section we compare the impacts of LCC as estimated with both methods in each of the analyzed LUCID models.

By design, the reconstruction method only computes the climate impacts of LCC over high-LCC grid cells. For comparison purposes, we therefore also consider these impacts according to the factorial experiment method over high-LCC grid cells only. We have computed them using two different sets of experiments forced by CO_2, SSTs, and sea ice reflecting either preindustrial or present-day background climate conditions (i.e., both PD − PDv and PIv − PI). However, consistently with de Noblet-Ducoudré et al. (2012), we have found small differences between these two estimates; therefore, here we only show the mean of them.

(i) Changes in albedo and latent heat flux

Figure 4 (as well as Figs. S6 and S7) compares the reconstructed regional mean impacts of LCC on seasonal mean albedo, latent heat flux (LH), and surface air temperature to those estimated by the factorial experiment approach. Using two-tailed t tests, we also looked at whether the impacts estimated by the factorial experiment method were significantly different from zero and whether those computed by the reconstruction method were significantly different from zero and from the noise induced by possible confounding factors of the method (e.g., CO_2).

Overall, there is a very good concordance between the domain-averaged estimates of both methods for albedo

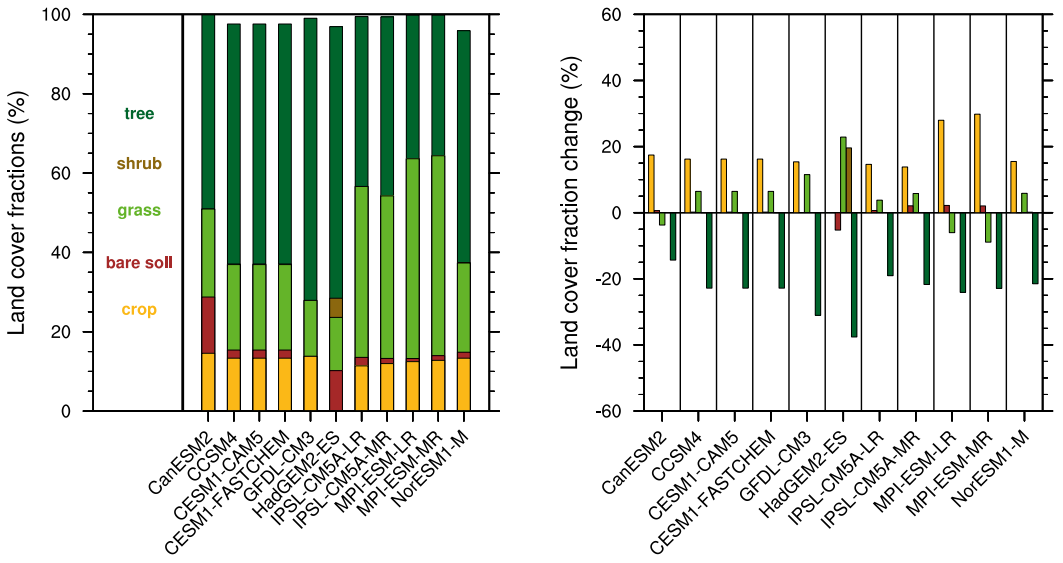

FIG. 3. As in Fig. 2, but for CMIP5 models.

and LH, as revealed by the high coefficients of determination of the regression lines between them (shown on the bar charts). The reconstruction method captures the sign as well as the seasonal cycle of the LCC impacts computed with the factorial experiment method. Besides, both methods almost always agree on the significance of the impacts and never show significant impacts of opposite signs. However, there is a systematic underestimation of the LCC impacts by the reconstruction method compared to the factorial experiment one, with the slopes of the regression lines ranging between 0.66 and 0.84. This can be expected from the design of the method, because it looks at differences between grid cells that underwent important LCC and others that underwent less important ones, whereas the factorial experiment method investigates differences between a world with and another without LCC. In addition to this, it could indicate that this difference due to the methodology is not compensated by positive feedbacks resulting from the interactions between LCC and the CO_2/SST/sea ice forcings, which would reinforce the impact of LCC in simulations where all forcings are simultaneously imposed.

(ii) Changes in surface air temperature

Overall, we see a good concordance between the two methods for seasonal mean temperature (see third panel of Fig. 4 and also Figs. S6 and S7). The reconstruction method captures the sign of the impacts estimated by the factorial experiments method for a majority of models and seasons. It also reproduces well the seasonal variations for the ARPEGE, IPSL and Simplified Parameterizations, Primitive-Equation Dynamics (SPEEDY) models. Differences in the sign of the LCC impacts may arise where these are equal to no more than 0.2°C, but in these cases at most one method shows significant results.

However, for almost all models and all seasons the LCC impacts on mean temperature are even more underestimated by the reconstruction method compared to the factorial experiment one than in the case of LH and albedo (the slopes of the regression lines can be as low as 0.37 over Eurasia). This suggests that the LCC-induced changes in temperature are less localized than those in land surface properties. In fact, if part of the local impacts on temperature over high-LCC grid cells had propagated to the neighboring grid cells that experienced less important LCC and that are located in the same bigger boxes, they would have been more underestimated by the reconstruction method than the impacts on albedo and LH. There is some modeling evidence supporting the fact that LCC can also affect temperature away from the perturbed areas, contrary to LH and albedo, which directly reflect the local characteristics of the land surface. The simulations of global-scale deforestation by Davin and de Noblet-Ducoudré (2010) showed that this is especially the case for the albedo-induced radiative cooling, which can propagate to other regions because it decreases temperature and hence humidity in the whole tropospheric column, whereas changes in surface roughness and evapotranspiration impact temperature mostly locally and close to the surface. The LCC-induced temperature changes over high-LCC grid cells may hence have partly propagated to the neighboring grid cells through the same mechanisms, even if we note that the overall good agreement between both methods indicates that they have mostly remained local.

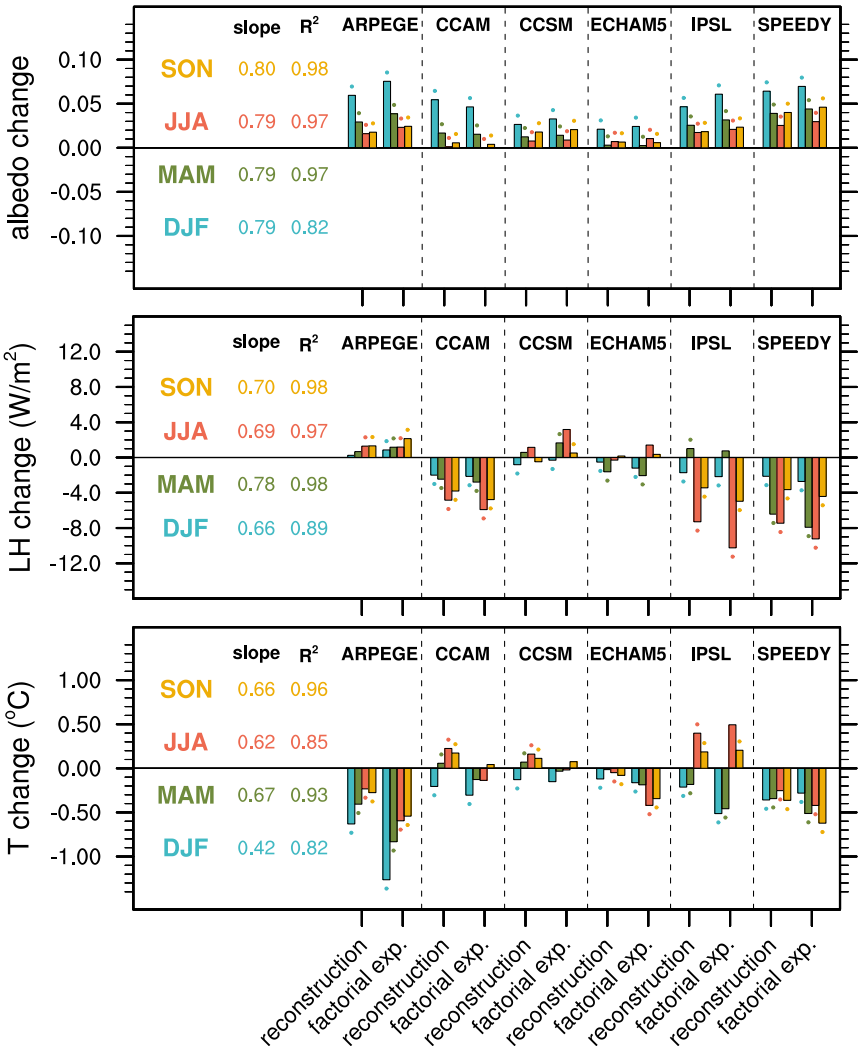

FIG. 4. Comparison of the reconstruction and factorial experiments methods showing LCC-induced changes in (top) albedo, (middle) latent heat flux, and (bottom) daily mean temperature over North America in LUCID models. The numbers on the left-hand side of each panel indicate the slopes of the regression line between the seasonal mean impacts diagnosed by the reconstruction vs the factorial experiments method, as well as the associated correlation coefficients. Dots indicate that results are statistically different from zero in the case of the factorial experiments method and statistically different from zero and the noise estimates in the case of the reconstruction method (at the 5% level, estimated with two-tailed *t* tests considering the spread between ensemble members).

We remark that our estimates of the impact of LCC according to the factorial experiment method may slightly differ from those of de Noblet-Ducoudré et al. (2012), because in their analysis they consider larger regions that include both high- and low-LCC grid cells. The potential larger-scale impact of the albedo-induced cooling (Davin and de Noblet-Ducoudré 2010) may play a more important role over low-LCC grid cells, which could explain why de Noblet-Ducoudré et al. (2012) reported a cooling effect of LCC in all seasons in the Conformal-Cubic Atmospheric Model (CCAM) and CCSM models for a larger domain in North America, whereas we computed a slight warming effect in SON over high-LCC grid cells only for these two models.

To conclude, we acknowledge that one advantage of the factorial experiment approach is its ability to assess the impacts of LCC in other regions than those that underwent important perturbations, whereas the reconstruction method focuses on the local consequences for the high-LCC grid cells. However, the reconstruction method is more appropriate to track what the effects of changes in a particular vegetation type are, even if it

cannot fully disentangle different land-cover transitions in its current design. Besides, we argue that one relative disadvantage of the factorial experiment method is that it may miss possible interactions between LCC and other forcings that are simultaneously imposed on the climate system. Although these have likely remained negligible in the LUCID simulations, because the small differences between the estimates of the factorial experiment method under either preindustrial or present-day conditions suggest that changes in background climate during the industrial period did not have a primary influence on the impacts of LCC, this may however be different in the future, when important changes in temperature are expected, especially on land (Pitman et al. 2011; Collins et al. 2013).

2) Signal-to-noise ratio of the reconstruction method

To assess to what extent possible confounding factors of the reconstruction method (e.g., other forcings and artifacts due to climatic gradients unrelated to LCC within the bigger boxes) may distort its estimates of the impacts of LCC, we apply it to the differences between LUCID experiments that are not forced by the same GHG concentrations, SSTs, and sea ice extents but share the same land-cover map. This enables us to quantify the noise of the method in these simulations: that is, climate changes that were extracted by the method even if they are not due to LCC. It can then be compared to the signal obtained when applying the method to the differences between simulations where all forcings are different (PD − PI), as this is the case for the analyzed CMIP5 simulations.

We computed the noise for all ensemble members and in both possible combinations of experiments (PD − PIv and PDv − PI). For each variable, we then compared the mean noise estimates to the mean signal computed from all ensemble members. Regarding albedo, the regional mean signal-to-noise ratios are equal to ~100 on average for all models and all seasons and are even seldom inferior to 10, for both North America (Fig. 5a) and Eurasia and South Asia (Figs. S8 and S9). This demonstrates the very good ability of the reconstruction method to disentangle regional mean albedo changes over high-LCC grid cells that are due to LCC from those due to its possible confounding factors. Only over a minority of individual grid cells is the signal not high enough to be distinguished from the noise. The domain-averaged ratios are also high for the latent heat flux, ranging mostly between 10 and 100 (Fig. 5b), except for some estimates where the reconstructed signal is low (i.e., ARPEGE and ECHAM5 in specific seasons over Eurasia and South Asia). For mean temperature, the regionally averaged ratios are typically equal to 10 and always exceed 2 (Fig. 5c), with the exceptions of ECHAM5 in JJA and SON over Eurasia and South Asia as well as IPSL in SON, for which the reconstructed signal is almost zero. This analysis demonstrates the overall good ability of the method to extract the regionally averaged impact of LCC on seasonal mean temperature in all-forcings simulations, given that this impact is large enough. It hence confirms that the basis assumption according to which LCC mostly affects grid cells individually whereas other forcings affect all grid cells within a bigger box in a rather similar way is verified. This therefore means that, even if the impact of LCC on temperature is not completely local, its spatial fingerprint is still smaller and distinguishable from that of other forcings. Besides, the presented signal-to-noise analysis shows that possible spurious signals due to climatic gradients unrelated to LCC only have a very limited influence on the diagnosed LCC impacts. In the next sections, we use these noise estimates to assess the significance of the reconstructed impacts in both LUCID and CMIP5 simulations. We acknowledge that other possible confounding factors that were included in CMIP5 simulations may increase the noise of the method (e.g., the aerosol forcing), but we are unfortunately not in possession of simulations that would enable us to test this hypothesis.

3) Sensitivity of the reconstruction method to the choice of parameters

We first tested the sensitivity of the computed impacts of LCC and of their signal-to-noise ratios to the choice of the threshold used to differentiate between high- and low-LCC grid cells, as well as to the size of the bigger box. For North America, we found that the choice of the threshold significantly affects the sign of the estimated impact of LCC only in one case, where it remains low (MAM LH in IPSL; see Figs. S10–S12). However, we find that selecting higher thresholds overall tends to increase the magnitude of the impacts with both methods, which is consistent with the fact that it implies a higher difference in the decrease in tree fraction between high- and low-LCC grid cells. Eventually, we selected the threshold of 15% as well as a varying bigger box approach, because for all models they enable us to avoid low signal-to-noise ratios and often even to maximize them (see Figs. S13 and S14), while keeping a reasonably high number of both high- and low-LCC grid cells.

We also remark that in a few cases we find a better agreement between estimates of both methods when the reconstruction is computed by discriminating land grid cells depending on the increase in crop cover they

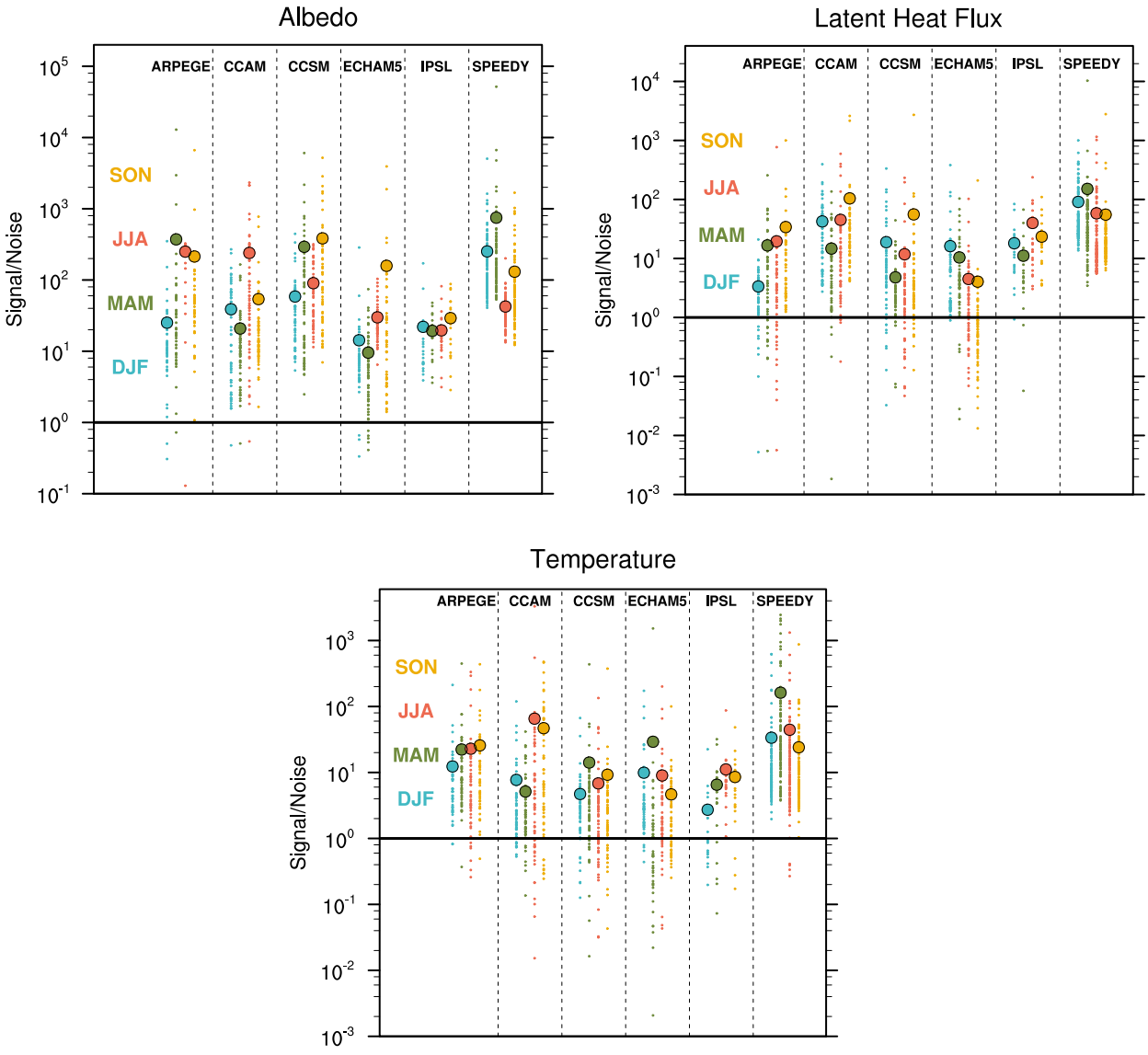

FIG. 5. Signal-to-noise ratios for seasonal mean albedo, latent heat flux, and daily mean temperature over North America in LUCID models. Small dots stand for individual grid cells, while big dots represent the domain-averaged signal-to-noise ratios.

experimented, rather than on the decrease in tree fraction (e.g., for temperature in the CCAM model, see Fig. S15). However, this is not a general rule, and we in contrast also find that basing the method on the decrease in tree fraction overall gives higher signal-to-noise ratios (Fig. S13).

b. Part 2: Reconstructed LCC effects in LUCID and CMIP5 models

1) SEASONAL MEAN ALBEDO

Most LUCID and CMIP5 models indicate that historical deforestation entailed an increase in albedo in all seasons (Fig. 6). Only CCAM, CanESM2, GFDL CM3, and MPI-ESM-LR show some nonsignificant changes in some seasons. For all LUCID models and 10 out of 11 CMIP5 models, the season where albedo increases most in North America and Eurasia is DJF because of the snow-masking effect. This is not the case in the subtropical South Asia domain; hence, we find lower LCC-driven albedo increases and no model agreement on a seasonal pattern there (Figs. S19–S21). Albedo changes over North America are, on average, ~30% higher in LUCID than in CMIP5 models (+0.045 on average in DJF and +0.012 in JJA, against +0.035 and +0.01 for CMIP5 models). We attribute this to differences in the vegetation maps because the decrease in tree fraction

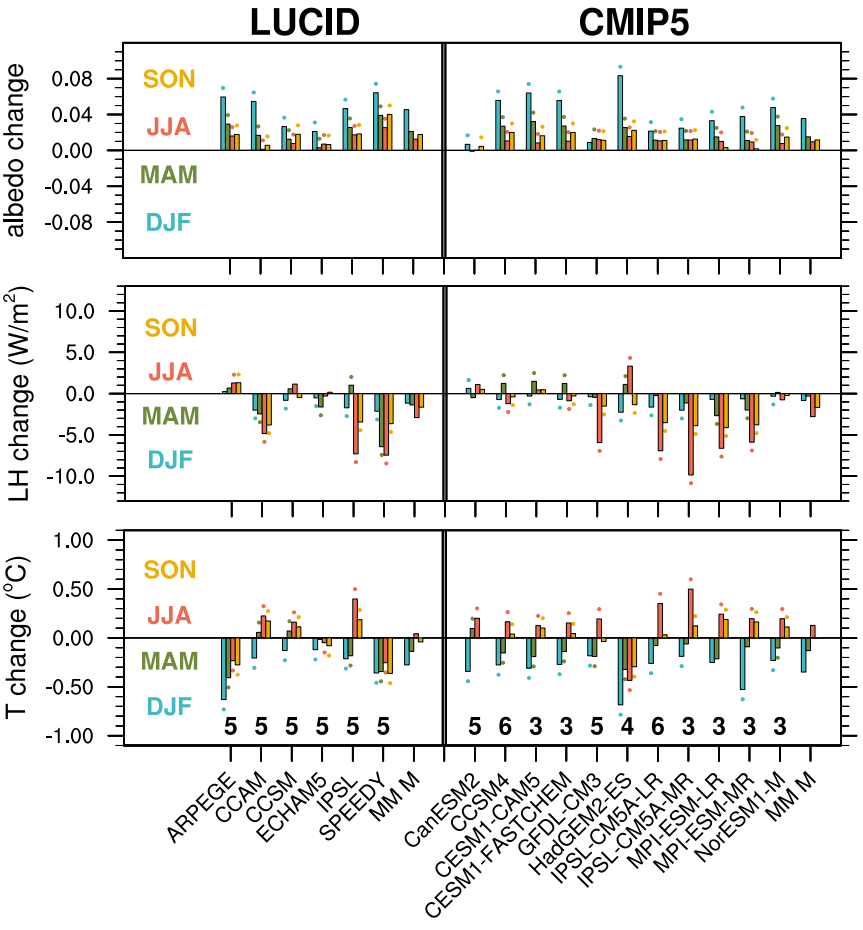

FIG. 6. Reconstructed impacts of LCC on seasonal mean (top) albedo, (middle) latent heat flux, and (bottom) temperature over North America in (left) LUCID and (right) CMIP5 models. The different colors refer to different seasonal averages. The number of ensemble simulations included in the analysis is indicated in black. LCC impacts are calculated based on the decrease in tree cover (threshold = −15). In the case of CMIP5, the multimodel mean (MM M) was computed by giving to the two models of the IPSL family and the two models from the MPI family only half a weight, while models including the CLM land surface model [CCSM4, CESM1(CAM5), CESM1(FASTCHEM), and NorESM1-M] were given only a quarter of a weight each. Dots indicate that results are significantly different at the 5% level from zero as well as from the noise estimates computed for each ensemble member (according to a two-tailed *t* test).

between high- and low-LCC grid cells is higher for LUCID models compared to CMIP5 ones (33% vs 25% of additional deforestation on average; see Figs. 2b and 3b). In contrast, we find no indication that the sensitivity of albedo to the deforestation rate is significantly different among LUCID and CMIP5 models (as estimated with a linear regression between albedo changes and the deforestation rates).

2) SEASONAL MEAN LATENT HEAT FLUX

A majority of LUCID and CMIP5 models simulate a decrease in LH due to deforestation, although the intermodel agreement is less clear than for albedo changes. We find impacts on LH of the same magnitude in LUCID and in CMIP5 models. They are maximal in JJA, with a multimodel mean reduction by between −2 and $-3\,\mathrm{W\,m^{-2}}$ over North America, while it ranges between −1 and $-2\,\mathrm{W\,m^{-2}}$ in SON and does not exceed $-1\,\mathrm{W\,m^{-2}}$ in DJF and MAM. However, LH increases in at least one season for 3 out of 6 LUCID models and 5 out of 11 CMIP5 models. The model disagreement is also strongest in JJA, during which CCAM, IPSL, and SPEEDY, as well as GFDL CM3, the two IPSL, and the two MPI models from the CMIP5 project show a decrease in LH by more than $4.5\,\mathrm{W\,m^{-2}}$, whereas ARPEGE and HadGEM2-ES show significant

increases in LH that even exceed 3 W m^{-2} in the case of the latter model.

Overall, the mean decrease in LH is consistent with the albedo-driven decrease in net radiation, but over North America albedo changes only explain 4% of the intermodel variance in the changes in LH in JJA for CMIP5 models (against 18% for LUCID models). This therefore suggests that CMIP5 models do not share a consistent response to the partitioning of available energy between the latent and sensible heat fluxes. This was already clearly reported in the context of the LUCID models (de Noblet-Ducoudré et al. 2012).

We find lower changes in LH over Eurasia and South Asia (see Figs. S18–S19 and S22–S23), which we at least partly relate to the lower differences in the decrease in tree fraction between high- and low-LCC grid cells experienced in these regions (−21% in the CMIP5 models and −29% in the LUCID ones in Eurasia, against −16% and −25% in South Asia, respectively). However, while we find a qualitatively similar model spread in Eurasia compared to North America, this is not the case for South Asia, where only ARPEGE simulates some significant increase in LH in DJF in response to historical LCC. This shows that there is a higher model agreement that evapotranspiration diminishes after a reduction in tree cover in subtropical and tropical regions.

3) SEASONAL MEAN TEMPERATURE

All models show that historical LCC entailed a cooling of the surface air temperature in winter in the midlatitudes. This cooling is significant for all but one model over North America (lower panel of Fig. 6) and for all but two models over Eurasia (Fig. S18). This demonstrates that the midlatitude winter cooling previously reported in LUCID studies is also a robust feature in the CMIP5 models. The multimodel mean cooling is of about −0.3° and −0.4°C over North America and −0.3° and −0.2°C over Eurasia for LUCID and CMIP5, respectively. We find that albedo changes are the dominating mechanisms for changes in surface air temperature in DJF when snow covers large areas and vegetation is mostly dormant, with 31% of the intermodel variance in LCC-induced temperature changes over North America being explained by changes in albedo (32% over Eurasia). The robust winter cooling is therefore consistent with the robust increase in albedo mentioned in a previous section.

In JJA, vegetation activity is highest and modifications of LH explain 32% of the intermodel variance in temperature over North America (16% over Eurasia), while the role of albedo is of a relatively lower importance (only 18% of the explained variance for North America and 11% for Eurasia). Consequently, there is less model agreement about the response of surface air temperature to LCC in the warm season. There are indeed as many LUCID models for which the reconstruction method indicates a significant cooling than a significant warming over both North America and Eurasia, with almost zero impact on average. As for CMIP5 models, the multimodel mean indicates an increase in surface temperature by ~0.1°C. Out of 11 models, 10 show a significant warming effect over North America and 5 over Eurasia, whereas only HadGEM2-ES shows a significant cooling effect in both regions. These results clearly show that, for a majority of CMIP5 models, during summertime high-LCC grid cells have warmed more than the surrounding areas during the industrial period. This also suggests a lower agreement about the regional-scale impact on surface air temperature (i.e., over all land grid cells) among CMIP5 models over midlatitudes, compared to what was concluded in LUCID studies.

Over both North America and Eurasia, the impact on surface air temperature in MAM and SON is intermediate between those in DJF and JJA for all models. Most of them indicate a cooling effect of LCC in MAM, which equals about 0.15°C on average over both regions. The impact in SON is often of the same sign as in JJA but of lower magnitude, and multimodel mean changes almost equal zero.

In the subtropical South Asian region, the increases in albedo and decreases in LH simulated by almost all models have counteracting effects on temperature, leading to model disagreement on the simulated impacts of LCC on this variable (Fig. S19). In contrast with the midlatitudinal regions, we find no clear seasonal pattern in this domain, with individual models often showing impacts of the same sign all year long.

c. *Part 3: Comparison of model results with observations*

In this section, we compare changes in surface air temperature simulated by the LUCID and CMIP5 models in response to historical LCC with present-day observations of the local effect of deforestation. Most of these observations purely rely on a spatial comparison between vegetation types, as opposed to our model analysis, which also emphasizes temporal changes. However, in agreement with de Noblet-Ducoudré et al. (2012), we found that changes in background climate during the industrial period did not have a primary influence on the effects of LCC, which means that present-day LCC should impact temperature in the same direction as those that have occurred since 1870. For these reasons, we expect present-day observations of the effect of deforestation to indicate what the sign of the reconstructed temperature response to simulated land-cover perturbations should be.

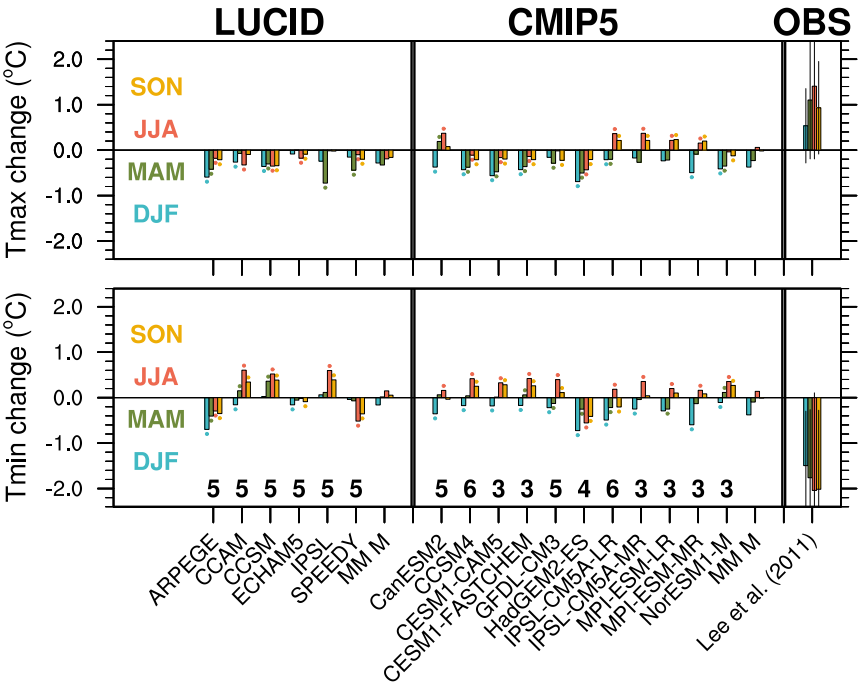

FIG. 7. Impacts of LCC on the diurnal cycle of temperature, according to historical reconstructions from LUCID and CMIP5 models and from present-day observations. (left), (center) As in the bottom panel of Fig. 6, but for (top) Tmax and (bottom) Tmin. (right) Observed difference in Tmax and Tmin between open land and forest, averaged over 22 paired sites in North America (data are from Lee et al. 2011). The vertical lines represent two standard deviations within the sites.

We used the observational data from Lee et al. (2011), who compared air temperature measurements over forest and open land sites located close to each other (~30 km on average) in the United States and Canada. Since they showed a clear contrasted effect of deforestation on daytime and nighttime temperature, we have investigated whether models are able to capture this feature. To do so, we selected 22 observational sites located within high-LCC grid cells for at least one of the analyzed models and computed the average difference in daily minimum (Tmin) and maximum (Tmax) temperature between forest and open land.

1) NIGHTTIME TEMPERATURE

The in situ observations indicate a cooling effect of deforestation during nighttime over midlatitudinal North America, whereas the ability of the models to reproduce this behavior strongly depends on the considered season (lower panel of Fig. 7). Open land is cooler than forests by almost 2°C on average throughout the year among the selected sites, with very few of them that depart from this behavior (see also Figs. 8 and 9). This has also been observed by Vanden Broucke et al. (2015) for three paired sites over western Europe. Besides, some studies investigated the impact of deforestation on remotely sensed land surface temperatures (LSTs), either by comparing pixels that are mostly covered with forests against those mostly covered with open land (Wickham et al. 2012; Peng et al. 2014; Zhao and Jackson 2014; Li et al. 2015) or by comparing areas over which the forest cover evolved differently over the observation period (Alkama and Cescatti 2016). These studies also show a cooling effect of deforestation during nighttime over temperate and boreal midlatitudes (e.g., Zhao and Jackson 2014; Li et al. 2015), although it is in some cases less pronounced (Peng et al. 2014; Alkama and Cescatti 2016). The reasons invoked for the lower nighttime temperatures over open land in these studies are its lower roughness length, which reduces turbulence and can thus bring less heat from the atmosphere to the surface if the boundary layer is stable (Lee et al. 2011), interactions between its lower evapotranspiration rates, cloud formation, and radiation, as well as variations in heat capacity (Peng et al. 2014; Vanden Broucke et al. 2015).

The amplitude of the reconstructed LCC effects on temperature from model simulations is lower than in the observations, which can be expected since it was obtained by comparing model grid cells that underwent

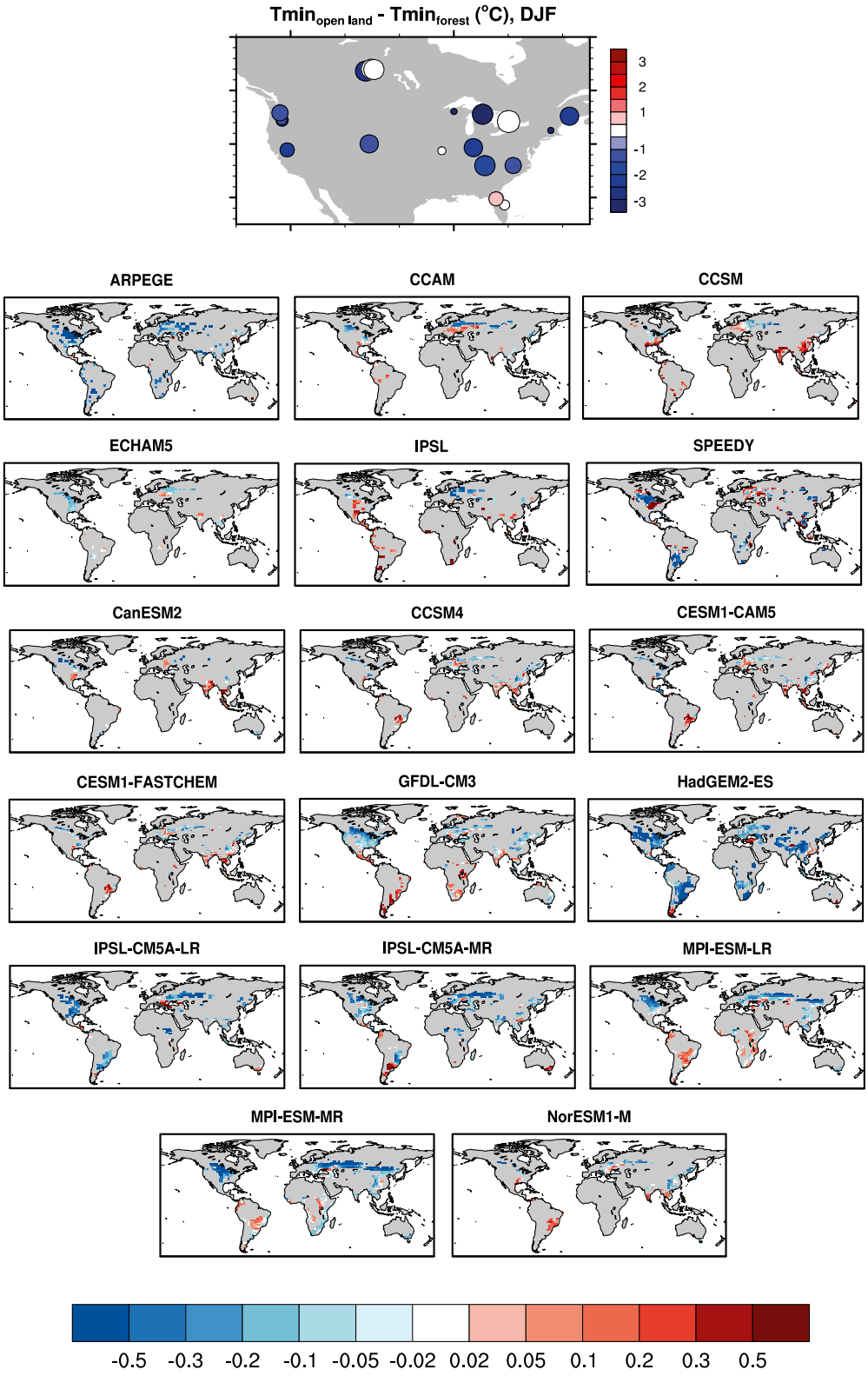

FIG. 8. (top) Difference in observed Tmin between open land and forest for the selected 22 paired sites from Lee et al. (2011). The color indicates the magnitude of the difference, while the size of the dot indicates the number of years (between three and 13). (bottom) Reconstructed DJF LCC impacts on Tmin for each model.

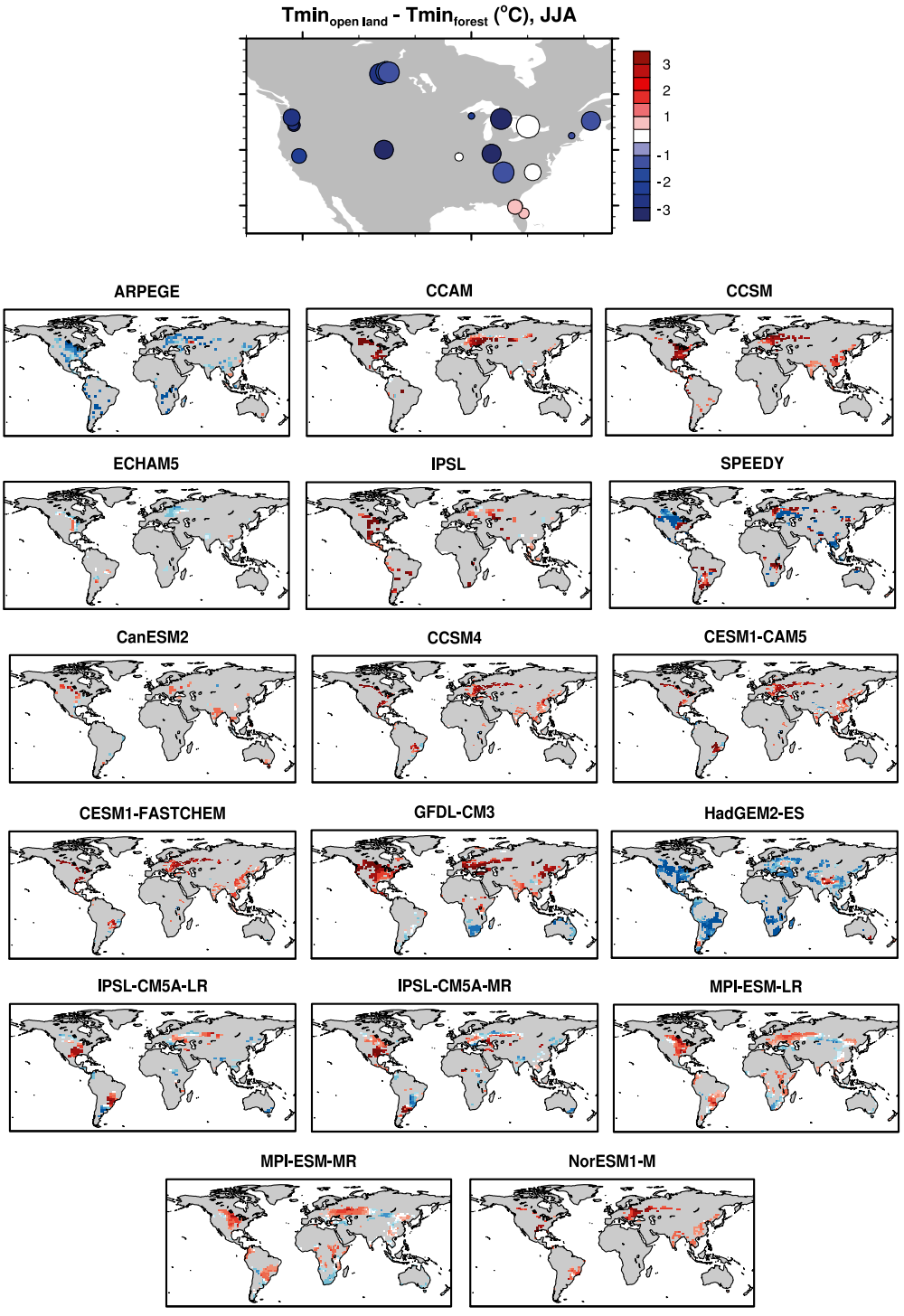

FIG. 9. As in Fig. 8, but for JJA.

partial deforestation, whereas observations intend to capture its full local effect. We find that, in agreement with observations, the 11 CMIP5 models simulate a significant decrease in Tmin in response to historical LCC during wintertime, while only three models out of six from the LUCID project reproduce this feature. In contrast, only one CMIP5 model (HadGEM2-ES) simulates a cooling of Tmin due to deforestation during summer, compared with two LUCID models (ARPEGE and SPEEDY).

2) DAYTIME TEMPERATURE

Contrary to their results for nighttime, the in situ observations overall show higher values of Tmax over open land compared to forests and especially during the warm season, when the multisite average indicates a daytime warming impact of deforestation by almost 1.5°C (higher panel of Fig. 7), while only a few sites experience the opposite behavior (Fig. 10). This effect is less strong in winter, with a multisite average increase in Tmax of about only 0.5°C over open land compared to forests and more spatially heterogeneous results (see also Fig. 11). The findings from Vanden Broucke et al. (2015) for Europe go in the same direction as those of Lee et al. (2011) regarding summertime; nonetheless, they show a slight cooling effect of deforestation in winter. Similarly, during summertime, Alkama and Cescatti (2016), Li et al. (2015), Zhao and Jackson (2014), Peng et al. (2014), and Wickham et al. (2012) found higher daytime LSTs over open land than over surrounding forests for midlatitudes but observed more contrasted results during wintertime, and especially latitudinal variations that the poorer spatial coverage of the in situ data may not allow one to capture. The higher daytime temperatures over open land during summer were explained by its lower roughness (Lee et al. 2011; Vanden Broucke et al. 2015) and its lower evapotranspiration rates (Peng et al. 2014; Li et al. 2015). This is counteracted by its higher albedo, which makes the difference in daytime temperature between open land and forests be almost zero during winter or at high latitudes (Lee et al. 2011) or even negative (Vanden Broucke et al. 2015; Li et al. 2015).

In light of these observational results, we conclude that on average CMIP5 models are performing better at simulating the warming effect of deforestation on Tmax during the warm season: five of them exhibit this feature in JJA and four during SON, while that is not the case for any of the LUCID models. All the analyzed models show a cooling effect of historical LCC during winter, which is significant for three models from LUCID and eight from CMIP5. This is in contrast with the results of Lee et al. (2011) but concurs more with the other previously mentioned observational studies.

Because of their contrasted results on the effect of midlatitudinal deforestation on daytime temperature, the various observational studies partly disagree on its impact on daily mean temperature. Consequently, this complicates the evaluation of the response of this variable to deforestation in the models presented in section 3b(3). However, these different pieces of observational evidence show more uniform conclusions regarding the effect of deforestation on the diurnal temperature range (DTR); therefore, we will now look at whether these are in agreement with model results.

3) DIURNAL TEMPERATURE RANGE

The in situ measurements indicate a diurnal asymmetry in the impact of deforestation on temperature over midlatitudes, which is more pronounced in summer. As a result, they show an increase in the DTR over open land compared to forests. This feature is also present in other observational studies and is particularly robust during the warm season. However, it contrasts very strongly with model results (Fig. 12 and Fig. S24 for Eurasia). In fact, none of the analyzed models simulate this behavior: about half of them actually show a reduction of the DTR in response to deforestation, while the other half suggest almost zero effect, on average, throughout the year, even if they may exhibit some small increases for specific seasons (e.g., SPEEDY or CanESM2 in summer, HadGEM2-ES in autumn, or IPSL-CM5A-LR in winter). Over South Asia, we find that only SPEEDY and CanESM2 simulate an increase in both Tmax and DTR and either a decrease or no change in Tmin during part of the year (Fig. S25). These two models hence better reproduce the observational results from Zhang et al. (2014), who extended the analysis of Lee et al. (2011). In particular, they included some sites located in tropical South Asia and South America, where they also observed higher Tmax over open land but similar Tmin values compared to forests. However, they report these features for the whole year, contrary to what SPEEDY and CanESM2 simulate. In general, we find that many models simulate a significant influence of deforestation on the seasonal cycle of surface air temperature. There is no robust evidence for this in the in situ observations, even if LST-based observational studies suggest that this may be the case for daytime at high latitudes.

This comparison between models and observations would need to be extended more thoroughly in order to confirm its findings. Especially, more extensive observational datasets should be included, since the reported studies make use of temporally limited data (between 3 and ~15 yr for the air temperature measurements; ~10 yr for the satellite observations), while the forest

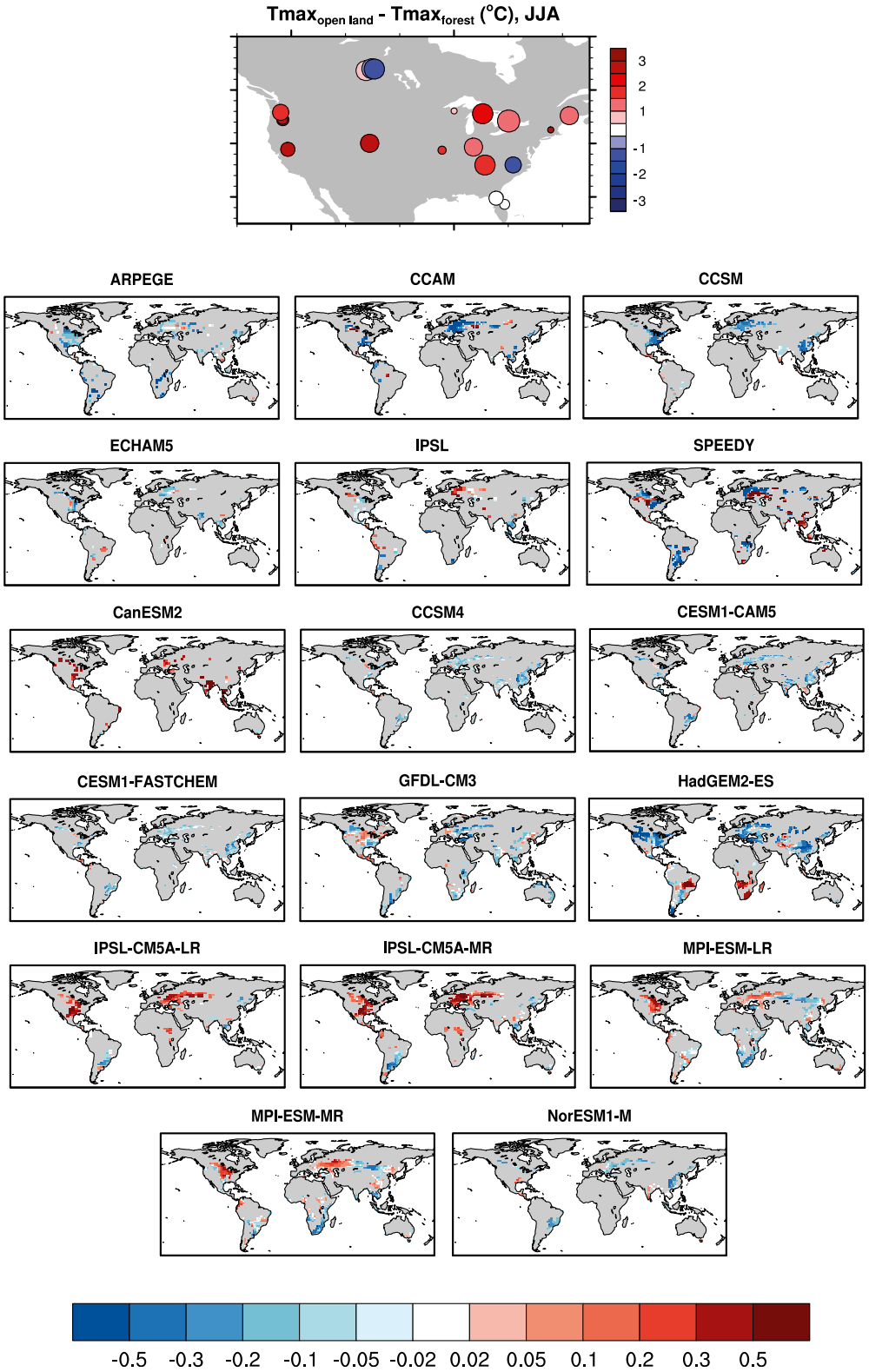

FIG. 10. (top) Difference in observed Tmax between open land and forest for the selected 22 paired sites from Lee et al. (2011). The color indicates the magnitude of the difference, while the size of the dot indicates the number of years (between 3 and 13). (bottom) Reconstructed JJA LCC impacts on Tmax for each model.

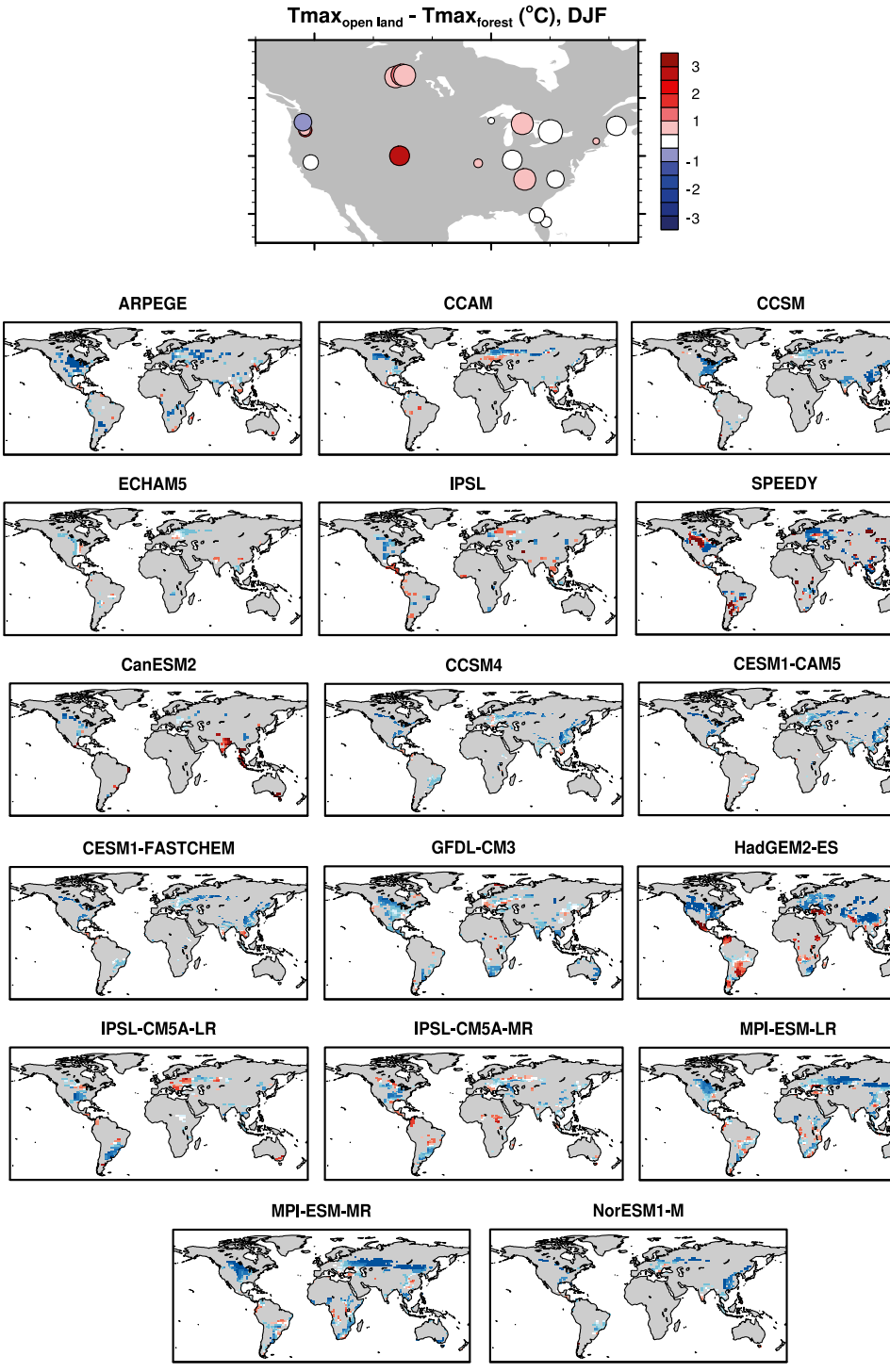

FIG. 11. As in Fig. 10, but for DJF.

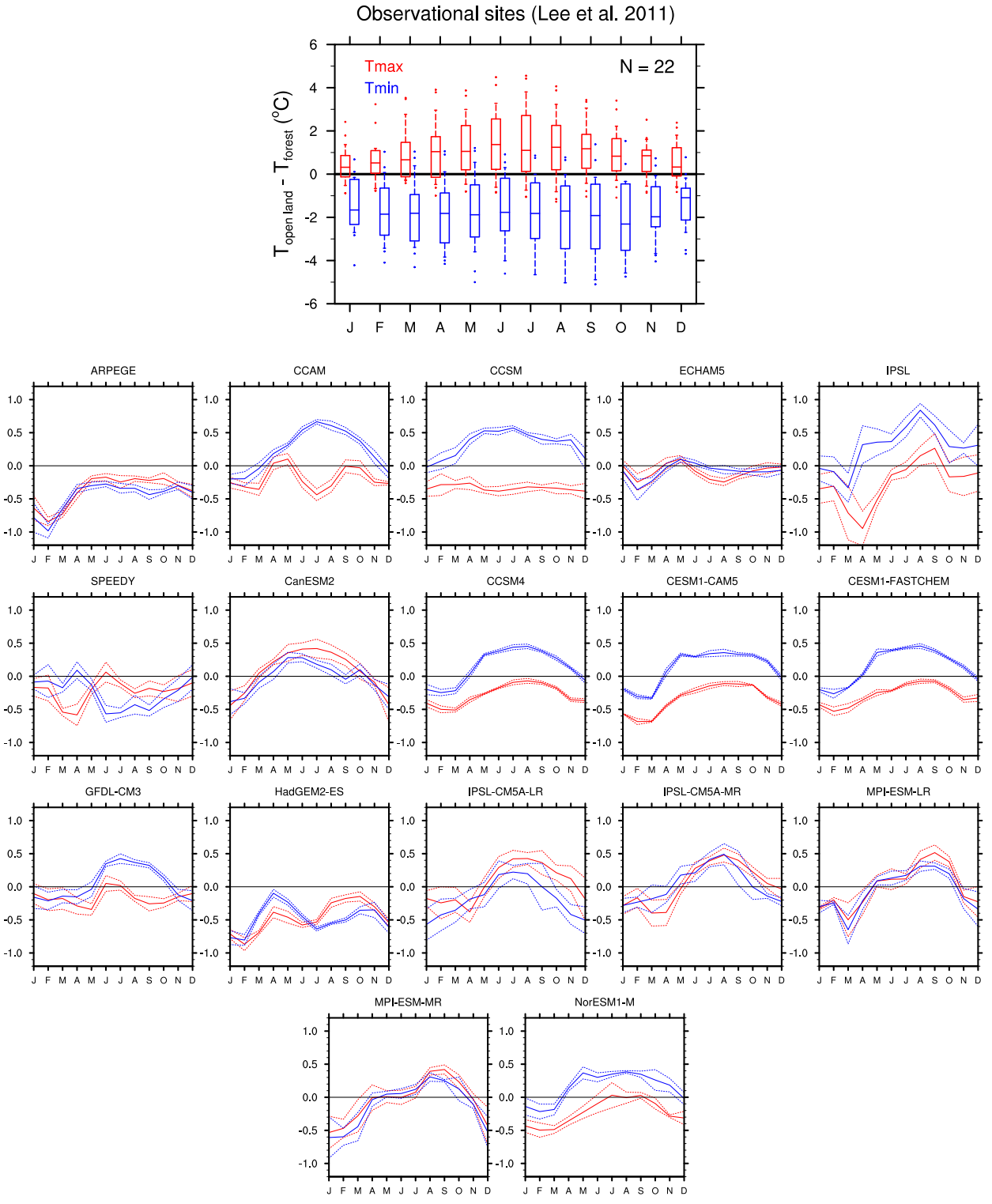

FIG. 12. (top) Seasonal cycle of the mean observed difference in daily maximum (red) and minimum (blue) temperatures between open land and forest over the selected 22 paired sites from Lee et al. (2011). The boxes indicate the interquartile range, while the whiskers show the range between the first and ninth deciles. (bottom) The seasonal cycle of the reconstructed LCC impact for six LUCID models and 11 CMIP5 models over North America. The full lines indicate the results for the ensemble mean, while the dashed lines represent the spread between ensemble simulations (two standard deviations). Note the different *y*-axis scale between the topmost plot and the others.

tower network used by Lee et al. (2011) also has a relatively poor spatial coverage. Furthermore, more research should be done to reconcile the contrasting pieces of evidence on the impact of deforestation on temperature on a daily average or during daytime in the cold season. However, this primary evaluation suggests that all the analyzed models have some deficiencies at representing the impact of deforestation on the diurnal cycle of temperature and thus highlights the need for more research to understand this poor performance.

4. Summary and conclusions

We reconstructed the historical impacts of LCC on albedo, latent heat flux, and surface air temperature using all-forcings simulations from the LUCID and CMIP5 model intercomparisons. To do so, we used a method comparing climate change signals over neighboring grid cells that experienced different rates of LCC but that were similarly affected by other historical climate forcings like CO_2.

First, using the LUCID simulations we showed that reconstructed estimates of LCC impacts compare well with results from factorial experiments explicitly isolating the LCC forcing. There is overall a very good concordance between the sign and the seasonal cycle of the LCC impacts estimated by both methods. We also found that, on average over the regions considered in this study, the impact of LCC on the analyzed variables can easily be disentangled from that of other climate forcings with the use of the reconstruction method.

Second, we compared the reconstructed historical LCC effects from both LUCID and CMIP5 models. We found that they agree on an increase in albedo due to historical LCC. This increase is maximal in winter because of the snow-masking effect and lowest in summer. On the contrary, there is more disagreement about the sign of the change in LH in summer and spring. While the multimodel means of both LUCID and CMIP5 model subsets indicate a decrease in LH that is consistent with the increase in albedo, individual models do not share a consistent response of the partitioning between latent and sensible heat fluxes. The agreement about albedo changes leads to a homogeneous cooling effect of LCC among all models during winter. However, since the response of evapotranspiration plays a more important role in summer, there is more disagreement about the impact on temperature in this season. Overall, a great majority of the analyzed models exhibit a local warming effect of LCC during summer, which contrasts with the results from previous LUCID studies.

In a third step, we compared our findings with observational evidence of the effect of deforestation on surface air temperature in North America. We find that none of the analyzed models are able to represent both the observed warming effect of deforestation during daytime in summer and its cooling effect during nighttime and, therefore, the resulting increase in DTR. Given the relative scarcity of observations of the effect of deforestation on climate and the existence of contrasting observational results regarding its impact during daytime in winter, this primary model evaluation needs to be extended. However, it already reveals some model deficiencies that need to be investigated in more detail, for example by a joint analysis of the effect of deforestation on changes in albedo, LH, and temperature in observations in order to disentangle the effects of different drivers of temperature changes and evaluate the representation of these mechanisms in models.

In conclusion, for the first time we demonstrated extensively the suitability of the employed reconstruction method to study the effects of temporal LCC on albedo, surface fluxes, and surface air temperature. We then used it to identify similarities and differences in the historical impacts of LCC as simulated by 17 GCMs from the LUCID and CMIP5 model intercomparison projects. Thereby, we found that some results from LUCID studies are confirmed, although substantial differences are also identified, especially regarding the impact of LCC during summertime. Besides, we extended this multimodel analysis with a comparison between model results and observations, which is to our knowledge new. This enabled us to highlight some fundamental issues with the representation of the LCC effects on the diurnal cycle of temperature in current land surface models. Nevertheless, it overall suggests that more recent CMIP5 models are closer to observations in that respect, hence underlining the positive effects of recent model developments.

Acknowledgments. We acknowledge partial support from the European Union through the projects FP7 EMBRACE (Grant Agreement 282672), H2020 CRESCENDO (Grant Agreement 641816), and ERC DROUGHT-HEAT (Contract 617518). We thank Victor Brovkin and an anonymous reviewer for their constructive comments on the manuscript. We also thank very much Juan Pablo Boisier, Ruth Lorenz, Nathalie de Noblet-Ducoudré, Andy Pitman, and all LUCID modelers for providing LUCID data, as well as Xuhui Lee and colleagues for making the observational data available. We also acknowledge the World Climate Research Programme's Working Group on Coupled Modeling, which is responsible for CMIP, and we thank the climate modeling groups who took part in this project for producing and making available their model output. For CMIP, the

U.S. Department of Energy's Program for Climate Model Diagnosis and Intercomparison provides coordinating support and led development of software infrastructure in partnership with the Global Organization for Earth System Science Portals. Besides, we are very grateful to Urs Beyerle for his management of the CMIP5 database at ETH. Finally, we also thank Chris Jones, Vivek Avora, Ingo Bethke, and Dave Lawrence for providing additional data from CMIP5 simulations.

REFERENCES

Alkama, R., and A. Cescatti, 2016: Biophysical climate impacts of recent changes in global forest cover. *Science*, **351**, 600–604, doi:10.1126/science.aac8083.

Ambrose, S. M., and S. M. Sterling, 2014: Global patterns of annual actual evapotranspiration with land-cover type: Knowledge gained from a new observation-based database. *Hydrol. Earth Syst. Sci. Discuss.*, **11**, 12 103–12 135, doi:10.5194/hessd-11-12103-2014.

Arora, V. K., and Coauthors, 2011: Carbon emission limits required to satisfy future representative concentration pathways of greenhouse gases. *Geophys. Res. Lett.*, **38**, L05805, doi:10.1029/2010GL046270.

Bentsen, M., and Coauthors, 2013: The Norwegian Earth System Model, NorESM1-M - Part 1: Description and basic evaluation of the physical climate. *Geosci. Model Dev.*, **6**, 687–720, doi:10.5194/gmd-6-687-2013.

Boisier, J.-P., and Coauthors, 2012: Attributing the impacts of land-cover changes in temperate regions on surface temperature and heat fluxes to specific causes: Results from the first LUCID set of simulations. *J. Geophys. Res.*, **117**, D12116, doi:10.1029/2011JD017106.

Brovkin, V., S. Sitch, W. von Bloh, M. Claussen, E. Bauer, and W. Cramer, 2004: Role of land cover changes for atmospheric CO_2 increase and climate change during the last 150 years. *Global Change Biol.*, **10**, 1253–1266, doi:10.1111/j.1365-2486.2004.00812.x.

Collins, M., and Coauthors, 2013: Long-term climate change: Projections, commitments and irreversibility. *Climate Change 2013: The Physical Science Basis*, T. F. Stocker et al., Eds., Cambridge University Press, 1029–1136. [Available online at http://www.climatechange2013.org/images/report/WG1AR5_Chapter12_FINAL.pdf.]

Collins, W. D., and Coauthors, 2006: The Community Climate System Model version 3 (CCSM3). *J. Climate*, **19**, 2122–2143, doi:10.1175/JCLI3761.1.

Collins, W. J., and Coauthors, 2008: Evaluation of the HadGEM2 model. Met Office Hadley Centre Tech. Note HCTN 74, 47 pp. [Available online at http://www.metoffice.gov.uk/media/pdf/8/7/HCTN_74.pdf.]

Davin, E. L., and N. de Noblet-Ducoudré, 2010: Climatic impact of global-scale deforestation: Radiative versus nonradiative processes. *J. Climate*, **23**, 97–112, doi:10.1175/2009JCLI3102.1.

de Noblet-Ducoudré, N., and Coauthors, 2012: Determining robust impacts of land-use-induced land-cover changes on surface climate over North America and Eurasia: Results from the first set of LUCID experiments. *J. Climate*, **25**, 3261–3281, doi:10.1175/JCLI-D-11-00338.1.

Dufresne, J.-L., and Coauthors, 2013: Climate change projections using the IPSL-CM5 Earth System Model: From CMIP3 to CMIP5. *Climate Dyn.*, **40**, 2123–2165, doi:10.1007/s00382-012-1636-1.

Findell, K. L., E. Shevliakova, P. C. D. Milly, and R. J. Stouffer, 2007: Modeled impact of anthropogenic land-cover change on climate. *J. Climate*, **20**, 3621–3634, doi:10.1175/JCLI4185.1.

Foley, J. A., and Coauthors, 2005: Global consequences of land use. *Science*, **309**, 570–574, doi:10.1126/science.1111772.

Ge, J., 2010: MODIS observed impacts of intensive agriculture on surface temperature in the southern Great Plains. *Int. J. Climatol.*, **30**, 1994–2003, doi:10.1002/joc.2093.

Gent, P. R., and Coauthors, 2011: The Community Climate System Model, version 4. *J. Climate*, **24**, 4973–4991, doi:10.1175/2011JCLI4083.1.

Hurtt, G. C., and Coauthors, 2011: Harmonization of land-use scenarios for the period 1500–2100: 600 years of global gridded annual land-use transitions, wood harvest, and resulting secondary lands. *Climatic Change*, **109**, 117–161, doi:10.1007/s10584-011-0153-2.

Klein Goldewijk, K., 2001: Estimating global land use change over the past 300 years: The HYDE database. *Global Biogeochem. Cycles*, **15**, 417–433, doi:10.1029/1999GB001232.

——, A. Beusen, G. van Drecht, and M. de Vos, 2011: The HYDE 3.1 spatially explicit database of human-induced land use change over the past 12,000 years. *Global Ecol. Biogeogr.*, **20**, 73–86, doi:10.1111/j.1466-8238.2010.00587.x.

Kumar, S., P. A. Dirmeyer, V. Merwade, T. DelSole, J. M. Adams, and D. Niyogi, 2013: Land use/cover change impacts in CMIP5 climate simulations: A new methodology and 21st century challenges. *J. Geophys. Res.*, **118**, 6337–6353, doi:10.1002/jgrd.50463.

Lee, X., and Coauthors, 2011: Observed increase in local cooling effect of deforestation at higher latitudes. *Nature*, **479**, 384–387, doi:10.1038/nature10588.

Li, Y., M. Zhao, S. Motesharrei, Q. Mu, E. Kalnay, and S. Li, 2015: Local cooling and warming effects of forests based on satellite observations. *Nat. Commun.*, **6**, 6603, doi:10.1038/ncomms7603.

Loarie, S. R., D. B. Lobell, G. P. Asner, Q. Mu, and C. B. Field, 2011: Direct impacts on local climate of sugar-cane expansion in Brazil. *Nat. Climate Change*, **1**, 105–109, doi:10.1038/nclimate1067.

Marsland, S. J., H. Haak, J. H. Jungclaus, M. Latif, and F. Röske, 2003: The Max-Planck-Institute global ocean/sea ice model with orthogonal curvilinear coordinates. *Ocean Modell.*, **5**, 91–127, doi:10.1016/S1463-5003(02)00015-X.

Marti, O., and Coauthors, 2010: Key features of the IPSL ocean atmosphere model and its sensitivity to atmospheric resolution. *Climate Dyn.*, **34**, 1–26, doi:10.1007/s00382-009-0640-6.

McGregor, J. L., and M. R. Dix, 2008: An updated description of the Conformal-Cubic Atmospheric Model. *High Resolution Numerical Modelling of the Atmosphere and the Ocean*, K. Hamilton and W. Ohfuchi, Eds., Springer, 51–75.

McPherson, R. A., D. J. Sternsrud, and K. C. Crawford, 2004: The impact of Oklahoma's winter wheat belt on the mesoscale environment. *Mon. Wea. Rev.*, **132**, 405–421, doi:10.1175/1520-0493(2004)132<0405:TIOOWW>2.0.CO;2.

Peng, S.-S., and Coauthors, 2014: Afforestation in China cools local land surface temperature. *Proc. Natl. Acad. Sci. USA*, **111**, 2915–2919, doi:10.1073/pnas.1315126111.

Pitman, A. J., and Coauthors, 2009: Uncertainties in climate responses to past land cover change: First results from the LUCID intercomparison study. Geophys. *Res. Lett.*, **36**, L14814, doi:10.1029/2009GL039076.

——, F. B. Avila, G. Abramowitz, Y. P. Wang, S. J. Phipps, and N. de Noblet-Ducoudré, 2011: Importance of background climate in determining impact of land-cover change on regional climate. *Nat. Climate Change*, **1**, 472–475, doi:10.1038/nclimate1294.

Pongratz, J., C. Reick, T. Raddatz, and M. Claussen, 2008: A reconstruction of global agricultural areas and land cover for the last millennium. *Global Biogeochem. Cycles*, **22**, GB3032, doi:10.1029/2007GB003153.

——, ——, ——, and ——, 2010: Biogeophysical versus biogeochemical climate response to historical anthropogenic land cover change. *Geophys. Res. Lett.*, **37**, L08808, doi:10.1029/2010GL043010.

Raddatz, T. J., and Coauthors, 2007: Will the tropical land biosphere dominate the climate–carbon cycle feedback during the twenty-first century? *Climate Dyn.*, **29**, 565–574, doi:10.1007/s00382-007-0247-8.

Ramankutty, N., and J. A. Foley, 1999: Estimating historical changes in global land cover: Croplands from 1700 to 1992. *Global Biogeochem. Cycles*, **13**, 997–1027, doi:10.1029/1999GB900046.

Roeckner, E., and Coauthors, 2006: Sensitivity of simulated climate to horizontal and vertical resolution in the ECHAM5 atmosphere model. *J. Climate*, **19**, 3771–3791, doi:10.1175/JCLI3824.1.

Salas-Mélia, D., and Coauthors, 2005: Description and validation of the CNRM-CM3 global coupled climate model. CNRM Working Note 103, 36 pp. [Available online at http://www.cnrm.meteo.fr/scenario2004/paper_cm3.pdf.]

Strengers, B. J., and Coauthors, 2010: Assessing 20th century climate–vegetation feedbacks of land-use change and natural vegetation dynamics in a fully coupled vegetation–climate model. *Int. J. Climatol.*, **30**, 2055–2065, doi:10.1002/joc.2132.

Taylor, K. E., R. J. Stouffer, and G. A. Meehl, 2012: An overview of CMIP5 and the experiment design. *Bull. Amer. Meteor. Soc.*, **93**, 485–498, doi:10.1175/BAMS-D-11-00094.1.

Vanden Broucke, S., S. Luyssaert, E. L. Davin, I. Janssens, and N. van Lipzig, 2015: New insights in the capability of climate models to simulate the impact of LUC based on temperature decomposition of paired site observations. *J. Geophys. Res. Atmos.*, **120**, 5417–5436, doi:10.1002/2015JD023095.

Wickham, J. D., T. G. Wade, and K. H. Riitters, 2012: Comparison of cropland and forest surface temperatures across the conterminous United States. *Agric. For. Meteor.*, **166–167**, 137–143, doi:10.1016/j.agrformet.2012.07.002.

Zhang, M., and Coauthors, 2014: Response of surface air temperature to small-scale land clearing across latitudes. *Environ. Res. Lett.*, **9**, 034002, doi:10.1088/1748-9326/9/3/034002.

Zhao, K., and R. B. Jackson, 2014: Biophysical forcings of land-use changes from potential forestry activities in North America. *Ecol. Monogr.*, **84**, 329–353, doi:10.1890/12-1705.1.